Available online at www.sciencedirect.com
SCIENCE DIRECT®
International Journal of Mass Spectrometry 243 (2005) 105–113
International Journal of Mass Spectrometry
www.elsevier.com/locate/ijms

Infrared multiphoton dissociation spectroscopy of protonated *N*-acetyl-alanine and alanyl-histidine

B. Lucas [a], G. Grégoire [a], J. Lemaire [b, c], P. Maître [b], F. Glotin [c], J.P. Schermann [a], C. Desfrançois [a, *]

[a] *Laboratoire de Physique des Lasers, UMR 7538 CNRS-Université Paris-Nord, Institut Galilée, Ave J.B. Clément, F-93430 Villetaneuse, France*
[b] *Laboratoire de Chimie-Physique, UMR 8000 CNRS-Université Paris XI, Bat. 350, F-91405 Orsay Cedex, France*
[c] *CLIO-LURE UMR 130 CNRS-CEA-Université Paris XI, Bat. 209D, F-91405 Orsay Cedex, France*

Received 10 December 2004; accepted 27 January 2005
Available online 26 February 2005

Abstract

Using Fourier transform ion cyclotron resonance mass-spectrometry (FT-ICR-MS) in combination with infrared multiphoton dissociation (IRMPD) spectroscopy, at the free electron laser (FEL) facility CLIO in Orsay (France), we obtain the IR spectra, in the 900–1900 cm^{-1} range, of two model protonated dipeptides: *N*-acetyl-alanine (AcNH-Ala) and alanyl-histidine (Ala-His). By comparison with simulated spectra, calculated at the B3LYP/6-31++G** level for many low-lying possible conformers of these two species, we are able to assign the position of the protonation site, on the acetyl oxygen for AcNH-Ala and on the side-chain imidazole nitrogen for Ala-His, and to obtain some more information on the low-lying equilibrium structures of these two species in the gas phase.

Keywords: IRMPD; Infrared spectroscopy; Protonated peptides; Frequency calculations

1. Introduction

The combination of infrared (IR) spectroscopy and mass-spectrometry (MS) is a powerful tool for the determination of molecular structures in the gas phase. MS allows the selection of the molecular species of interest and the measurement of their vibrational frequencies allows the discrimination between the different possible geometrical structures, through the comparison with quantum chemistry calculations or previous experimental data on similar systems.

When neutral systems are investigated, the ionisation process must as less perturbative as possible, in order to restrict fragmentation so that mass-spectra reflect as much as possible the neutral distribution. For molecular systems possessing a natural or artificial chromophore, with a well-resolved spectrum in the visible/UV region, ionisation can be achieved by means of a two-step resonant electronic excitation, via the well-known resonantly enhanced multiphoton ionisation (REMPI) technique. If a resonant IR excitation depopulates the lowest vibrational states, turning the first excitation photon off resonance, a dip appears in the cation signals. This IR/UV double resonance technique has been applied to several model biomolecules [1–6]. When there is no chromophore, an alternative ionisation method is available if the investigated neutral systems possess dipole moments large enough to capture very low-energy electrons. So-called dipole-bound anions, which structures are the same as those of their neutral parents, are then created and mass-selected. Resonant IR excitation of neutrals is then monitored though the observation of dips in the anion signals due to vibrationally induced electron autodetachment or predissociation of neutral complexes [7]. In both cases, neutral resonant IR excitation precedes ionisation that is also selective with respect to the molecular conformation, so that the obtained IR spectrum reflects only one neutral equilibrium structure.

* Corresponding author. Tel.: +33 149403723; fax: +33 149403200.
E-mail address: desfranc@lpl.univ-paris13.fr (C. Desfrançois).

1387-3806/$ – see front matter © 2005 Elsevier B.V. All rights reserved.
doi:10.1016/j.ijms.2005.01.002

For ionic molecular species in the gas phase, MS allows selecting directly the species of interest but resonant IR absorption can be detected only via fragmentation, since ion densities are too low for direct absorption measurements. For covalently bound molecular systems, one-photon linear absorption does not bring enough internal energy for efficient dissociation, so that one has to consider either non-covalent complexes or multiphoton techniques. In the first case, a weakly bound neutral messenger is attached to the ions and its evaporation is the signature of IR absorption [8–10]. When using rare gas atoms, this messenger favours the cooling of the molecular ions and introduces only minor modifications in their IR spectrum. In the second case, the ions are generally trapped for some time so that they can absorb several IR photons on the same vibrational transition, while each IR excitation spreads over other modes, by intramolecular vibrational relaxation (IVR), in between two photon absorption. IR multiphoton dissociation (IRMPD) then corresponds to a sequential absorption of IR photons that increases the internal ion energy above the dissociation limit, so that vibrational excitation is monitored through observation of mass-identified charged fragments. IRMPD experiments were initially performed with monochromatic or line-tuneable sources, e.g., CO_2 lasers [11–13], and more recently with high-power widely tuneable IR sources, e.g., free electron lasers (FEL) [14–16]. Resonant excitation of vibrational frequencies is thus now possible over a wide spectral range and this improves considerably the spectroscopic capabilities of the IRMPD method.

The here presented experimental results concern small protonated peptides [17–19] trapped in an ICR cell. Ions are thermalised at room temperature and the rotational distribution is such that the spectral linewidth of the vibrational absorption lines are comparable to those obtained for neutral species at room temperature [20]. This is in contrast with well-resolved spectra obtained for cold neutral species in supersonic expansions or for ions trapped at low temperatures. Thus, narrow-band IR sources, such as OPOs, do not necessarily present the best spectral matching and the present data have been obtained with the high-power broadly tuneable CLIO FEL facility in Orsay. This study is the continuation of a systematic investigation of protonation sites of small peptides by means of IRMPD. Our first study concerned dialanine for which we spectroscopically assigned the proton site on the terminal amino group and the *trans* amide conformation as the favoured structures. We here investigate protonated *N*-acetyl-alanine (AcNH-Ala), i.e., a protected dipeptide in which there is no more terminal amino group, and protonated alanyl-histidine (Ala-His), a dipeptide containing a basic side-chain on which the extra proton could be located.

2. Experimental

The IRMPD spectra of protonated peptides have been obtained with the CLIO FEL coupled to our home-built and mobile Fourier transform ion cyclotron resonance mass spectrometer (FT-ICR-MS) MICRA [21], as already described in our previous report [22]. We here only recall the main aspects of the experimental procedure and give some more specific details. The ICR cell operates with a permanent magnet that produces a magnetic field of 1.25 T, which limits the mass-range to 1000 amu. The protonated peptides are produced by matrix-assisted laser desorption ionisation (MALDI), from 0.5 mm thick pellets that are produced from a mixing of the CHCA (α-cyano-4hydroxycinnamic acid) matrix with either AcNH-Ala or Ala-His, in a 1:1 ratio. Amounts of 50 mg each are required to obtain a pellet solid enough to be easily manipulated and to resist to more than 2000 desorption laser shots that are necessary to obtain a full IRMPD spectrum. For desorption, the pulsed output beam of a Nd:YAG laser is frequency-tripled and irradiates the pellets without focusing. The target is mounted 6 mm away from the entrance trapping plate of the ICR cell and is maintained at 1.8 V, while a 3.5 V potential is applied to the trapping plates. The ions enter the ICR cell collinearly with the magnetic field through a 5 mm diameter hole drilled in the entrance trapping plate that is pulsed down to 0 V during 30–50 μs after the desorption laser shot. Cations produced in the MALDI plume possess large amounts of internal energy and are thus allowed to relax close to room temperature through collisions with the residual gas (few 10^{-8} Torr) or by black-body radiative exchange, during 2.4 s for AcNH-Ala and 1 s for Ala-His. Protonated cations at the mass of interest (132 amu for AcNH-Ala and 227 amu for Ala-His) are selected by ejection of all other ions and are further submitted to IR irradiation during 2 s. The FEL was operating at electron energies of 40–42 MeV, leading to a maximum average power of about 1 W at 9–10 μm and 0.4 W at 5–6 μm. However, both experiments were performed with one attenuator that divides by 3 the laser fluence, in order to avoid saturation. Considering the variation of the waist, as a function of the FEL power, the IR fluence is expected to be about the same from 5 to 10 μm [22] so that no fluence correction has been applied on the dissociation spectra. If F is the sum of the fragment ions produced by IRMPD and P, the number of intact parent ions, for a given photon energy E, the fragmentation yield is $F/(F+P) = 1 - \exp[-k(E)t]$, where $k(E)$ is the fragmentation rate and t, the irradiation time. Because the fragmentation yield was quite high, we rather plot the quantity $-\ln(1-(F/(F+P)))$ that is proportional to the fragmentation rate.

3. Results and discussion

3.1. Method

IRMPD is a multi-step absorption process that is possible due to fast IVR in between two IR photon absorptions [23,24]. A first IR photon is resonantly absorbed when its frequency coincides with that of the fundamental frequency of a vibrational mode i. Due to anharmonic couplings be-

tween vibrational modes, this excess energy can be quickly redistributed among other modes, so that the ion is back into the fundamental vibrational state of mode *i*. Due to this fast IVR, the excited ion can again absorb a photon resonant with the fundamental of mode *i*, while others modes acquire more and more vibrational energy. After several such steps, the ion internal energy is high enough for allowing ion dissociation. The FEL temporal structure is well suited for such process: the CLIO laser delivers series of 8 μs long macropulses composed of 500 micropulses that are separated by 16 ns. This time delay is large enough for IVR to occur, so that parent ions can easily absorb several photons within the same macropulse, without enough time for relaxing by radiative emission or by collision. IRMPD spectroscopy thus allows the experimental determination of fundamental frequencies of vibrational modes that can be compared to predictions of quantum chemistry calculations. However, as discussed in previous studies [7], the multiphoton process inherent in IRMPD can induce a slight red-shift in the position and some broadening of the absorption lines, together with some discrepancies in the intensities. Also, the temperature of the ions leads to a rotational bandwidth of about 40 cm^{-1} that is typical for such molecular species at room temperature.

Concerning the present calculations, our method was as follows. A first systematic search of possible conformations is first conducted at the semi-empirical AM1 level, using the conformational search procedure of the commercial software package HyperChem 7.0 (Hypercube Inc.). We then perform full structure optimisations, first at the B3LYP/6-31G* level, and then with the larger 6-31++G** basis set for the lowest-energy conformations. At this last level of theory, we can expect to predict rather accurate structures, energies and harmonic vibrational frequencies. Since ions are supposed to be cooled down close to room temperature before IR irradiation, we discuss their stabilities in terms of the calculated relative free energies at room temperature, which are to be compared with the typical energy per mode $kT \sim 0.6$ kcal/mol. For each possible conformation, the experimental IRMPD spectrum is compared with the calculated spectrum that is obtained after a scaling of the harmonic frequencies and a convolution with a 40 cm^{-1} wide Lorentzian profile, in order to take into account the rotational bandwidth. The frequency scaling factor we use is 0.975, for the whole spectrum, and has been determined from the previously studied protonated dialanine and corresponds to the best fit of the calculated frequencies to the experimental data for the two lowest-energy conformations [22]. The conformations are classified according to the possible protonation site of the considered peptide, with a nomenclature similar to our previous work [25].

3.2. Protonated N-acetyl-alanine

From the parent ion at $m/z = 132$, four fragment ions are observed, at $m/z = 114$, 90, 86 and 44, which correspond to losses of H_2O, CO, and CH_2CO. The first two fragments are the most dominant ones but all fragments possess almost

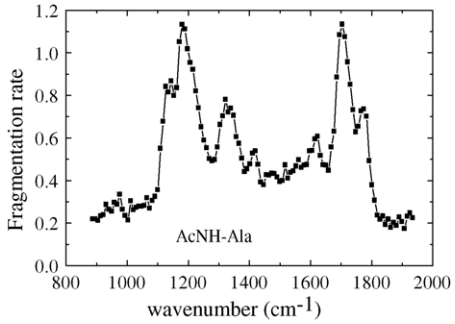

Fig. 1. Fragmentation rate of the protonated *N*-acetyl-alanine ions, as a function of the IR photon energy.

the same spectral dependency, even if the CH_3–CH=NH_2^+ immonium ion ($m/z = 44$) is more produced than the others around 1100–1250 cm^{-1}. Taking into account the sum of all these fragment ions, the plot of the dissociation rate $k(E)$ is displayed in Fig. 1, as a function of the photon energy. Three intense and broad peaks are observed at 1180, 1330 and 1700 cm^{-1}, together with four other peaks with weaker intensities at 1140, 1420, 1620 and 1770 cm^{-1}.

In AcNH-Ala, only three protonation sites are available, since there is no more terminal amino group. Isomers are, respectively, labelled by O, if the protonation site is on the acetyl oxygen, by D when it is on the peptide nitrogen, and by G for the carboxylic oxygen of the C terminus. In this latter case, protonation leads to a cyclic diol conformer, with a valence bond formed between the acetyl oxygen and the C terminal. The numbering following the proton site letter corresponds to the energy order in which the conformations have been found in the AM1 calculations. The B3LYP/6-31++G** calculated energies of the main equilibrium conformations are given in Table 1, among which some of the lowest-energy structures

Table 1
Energetics of the protonated AcNH-Ala conformers, calculated at the B3LYP/6-31++G** level

Conformer	ΔE_{ZPE}	ΔE_{298}	ΔG_{298}
O1	0	0	0
O2	0.33	0.30	0.36
O6	1.55	1.78	1.23
O7	3.66	3.97	3.11
*cis*O14	4.65	4.92	4.17
O11	5.11	5.40	4.65
O3	5.79	5.94	5.58
*cis*O5	5.36	5.61	4.97
*cis*O13	6.05	6.30	5.54
O12	5.60	5.95	4.74
O15	6.14	6.39	5.87
O4	7.66	7.83	7.34
O21	7.85	7.83	8.00
G2	10.15	10.02	10.78
D1	15.74	16.11	14.51

E_{ZPE} is the ZPE-corrected electronic energy at 0 K, while E_{298} is the electronic + thermal energy and G_{298} is the free energy at room temperature. The relative energy values (kcal/mol) are given with respect to the most stable conformation O1 that has the following energies: $E_{ZPE} = -476.646100$ a.u., $E_{298} = -476.636339$ a.u. and $G_{298} = -476.681270$ a.u.

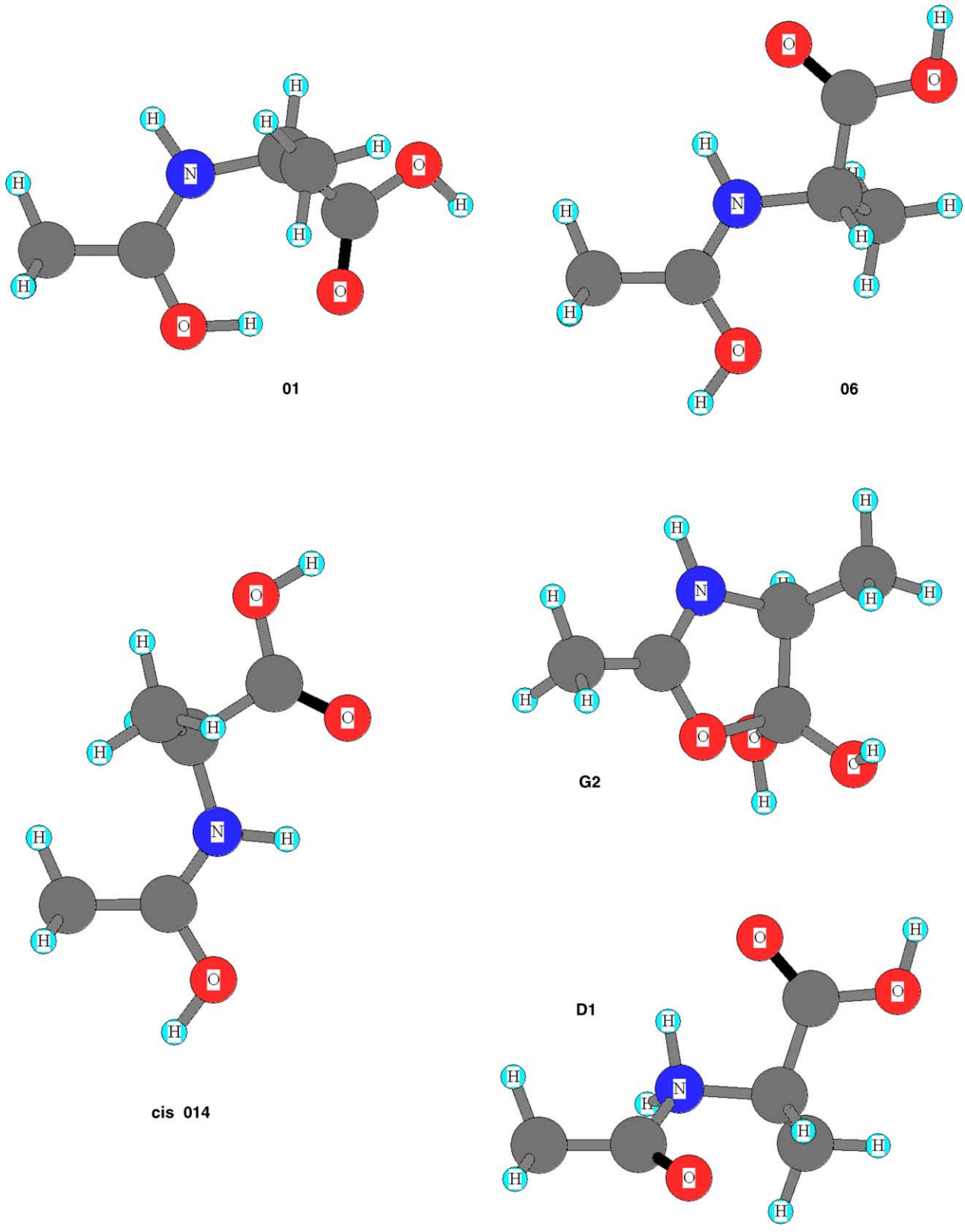

Fig. 2. Some of the most stable conformations of protonated *N*-acetyl-alanine ions. See text for the labelling and some discussion.

are displayed in Fig. 2, together with the corresponding simulated spectra in Fig. 3. Although D1 and G2 conformers possess high energies, thus they should not appear in the ion population, we display the corresponding results in order to show how much they differ from the low-lying O conformers. Their simulated spectra indeed differ very much from the experimental spectrum, particularly in the amide I region corresponding to the C=O stretch region. In G conformers, there is no more carbonyl group and thus there is no line in between 1650 and 1800 cm^{-1}, while in D conformers, the acetyl C=O group is free from H-bonding so that the corresponding line is calculated to be close to 1900 cm^{-1}. Other strong discrepancies also appear in the 1100–1200 cm^{-1} region, corresponding to various bending modes. It seems thus clear that the protonation site in AcNH-Ala can only be the acetyl oxygen in O conformers.

Among the different most stable O conformers, three of them are expected to be populated when the ions are thermally equilibrated around 300 K. Those are O1, O2 and O6 conformers that lie within less than 2 kcal/mol. Since O1 and O2 possess very similar structures, energies and spectra, only O1 and O6 results are displayed. The protonated O–H bond forms a strong H-bond with the carboxylic acid oxygen in O1, while it is directed towards the methyl group in O6 (and O14, see below). None of these two individual spectra really fit the experimental spectrum: in the O1 spectrum, two lines at 1330 and 1770 cm^{-1}, are missing that can be found in the O6 spectrum but then the line at 1620 cm^{-1} lacks. These complementary spectra suggest that the experimental spectrum could result from the superposition of the contribution of the three low-energy conformers. The experimental line at 1770 cm^{-1} then appears to correspond to the almost-free acid C=O stretch of O6 conformer, which is calculated at 1779 cm^{-1}. On the other hand, the line at 1700 cm^{-1} probably results from the superposition of the acid C=O stretch of O1, which is red-shifted by its H-bond interaction with the protonated O–H bond and which calculated value is 1723 cm^{-1}, with the almost-free acetyl C–O–H^+ bending of O6, which is not H-bonded and which calculated frequency is 1670 cm^{-1}. It must be noticed that, for both O1 and O6, the intense double peak at 1140–1180 cm^{-1} is not well reproduced. We have checked that higher-energy conformers give even worse spectra, as illustrated by the O14 spectrum, which corresponds to a *cis* conformation of the peptide bond. There, the low-frequency region may be better fitted, but the 1300–1600 cm^{-1} range is very far from the experimental data and the amide I region, especially the frequency difference between the two lines, is less well reproduced than in the O6 spectrum.

If the conformer population would follow a simple Boltzmann law at room temperature, we could expect 60% in the O1 conformer, 32% in the O2 conformer, only 7% in the O6 conformer and less than 1% for the others. However, the above comparison suggests that conformer O6 noticeably contributes also to the experimental spectrum. It may be that the cooling time is not long enough in these experiments

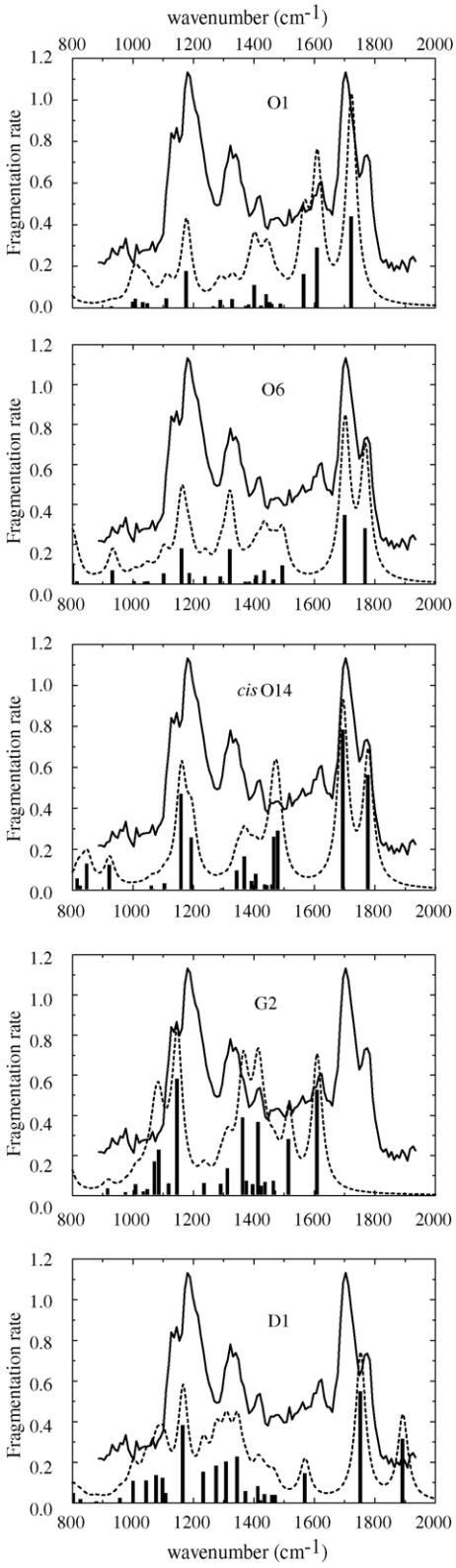

Fig. 3. Comparison between the experimental spectrum and the simulated spectra for the lowest conformers of protonated AcNH-Ala that are displayed in Fig. 2. See text for discussion.

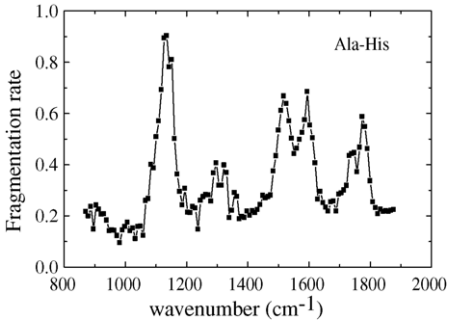

Fig. 4. Fragmentation rate of the protonated alanyl-histidine ions, as a function of the IR photon energy.

so that ions are still "trapped" in this configuration and that its population is larger than it would be expected from simple energetic considerations. In any case, the protonation site in AcNH-Ala is clearly the carbonyl oxygen of the acetyl group.

3.3. Protonated alanyl-histidine

From the parent ion at $m/z = 227$, the major fragment due to IRMPD is observed at $m/z = 209$ and corresponds to a loss of one water molecule. A second weaker fragment at $m/z = 110$ is also detected, with a similar spectral dependency, and is thus included in the total fragmentation yield. The obtained IRMPD spectrum is displayed in Fig. 4. A broad intense spectral line is observed at 1130 cm^{-1} (FWHM = 60 cm^{-1}) together with two other broad and intense bands at 1520 and 1595 cm^{-1}, while two rather weak amide I lines appear at 1740 and 1775 cm^{-1}. Around 1300 cm^{-1}, there is also one even weaker doublet, at 1295 and 1320 cm^{-1}, with may be to satellite lines on both sides, at 1260 and 1360 cm^{-1}.

A comparison between this experimental spectrum and simulation calculations is displayed in Fig. 5, for different lowest-energy conformers that are represented in Fig. 6. In protonated Ala-His dipeptide, there are six possible protonation sites. The proton can be on the terminal amino group (isomers A), on the oxygen of the terminal carboxylic acid group (isomers G), on the oxygen (isomers O) or the nitrogen (isomers D) of the amide bond, or on the nitrogen (isomers N) or the N–H group (isomers NH) of the side-chain imidazole ring. Since the proton affinity of the amino acid histidine is larger than that of alanine [26], it is expected that the N conformers should be favoured over the A conformers.

From the calculated energetics of Table 2, it is clear that NH, G and D conformers, and to a less extend also O conformers, are located at high energies as compared to A and N conformers. We here present only the lowest energies (O4, D1, G3 and NH1) of these four high-energy conformer types that are very unlikely to be present in the experiment and which simulated spectra are all far from the experimental one. As an example, we display the calculated spectrum and the geometry (Figs. 5 and 6) only for the lowest O4 configuration. As expected, the N conformers (protonation on the imidazole nitrogen) are calculated to be more stable than

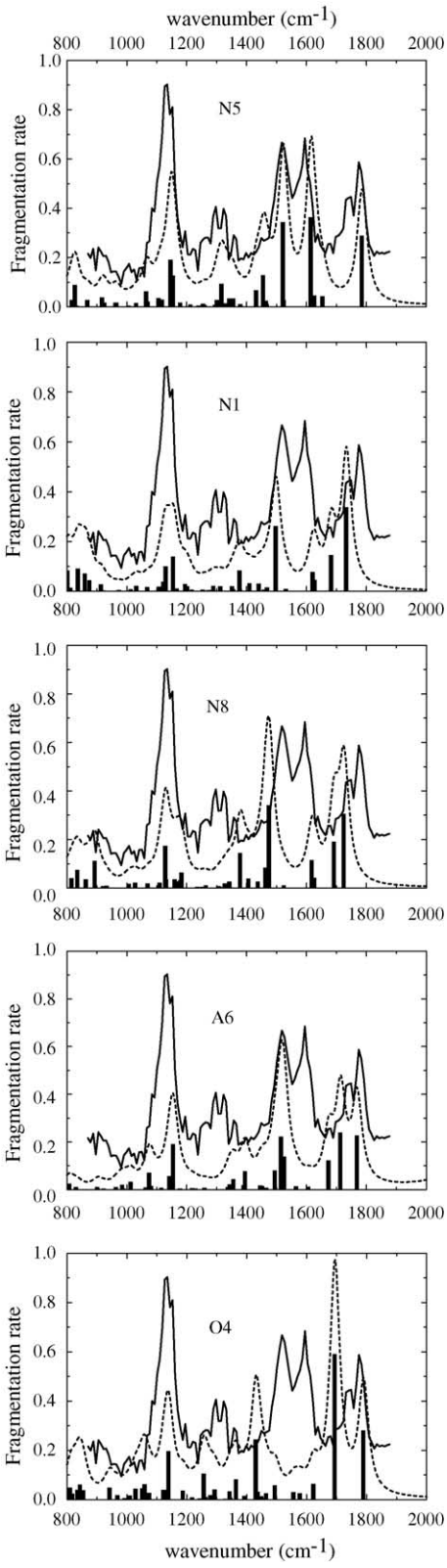

Fig. 5. Comparison between the experimental spectrum and the simulated spectra for the some of the lowest conformers of protonated Ala-His. See Fig. 6 for structures and text for discussion.

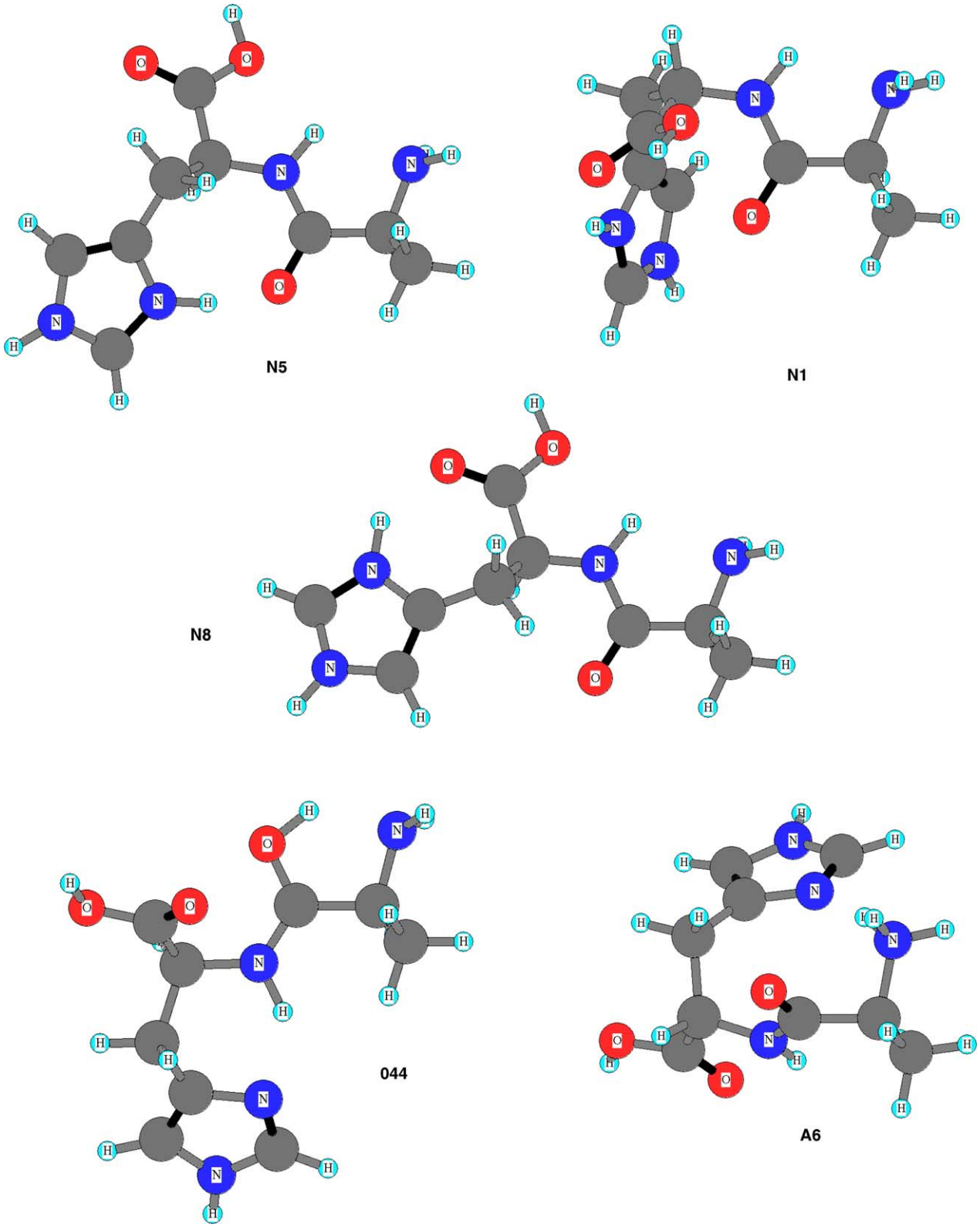

Fig. 6. Structures of some of the most stable conformations of protonated alanyl-histidine, corresponding to the simulated spectra of Fig. 5. See text for labelling.

Table 2
Energetics of the protonated Ala-His conformers, calculated at the B3LYP/6-31++G** level

Conformer	ΔE_{ZPE}	ΔE_{298}	ΔG_{298}
N5	0	0	0
N7	0.79	0.83	0.71
N1	3.31	3.30	3.79
N2	3.57	3.65	3.59
N8	4.89	5.04	4.51
N4	4.97	5.09	4.71
A6	5.61	5.38	6.71
N10	7.26	7.39	6.84
A7	8.30	8.13	9.10
*cis*A1	9.45	9.26	10.53
O4	10.14	10.16	10.20
D1	18.41	18.41	18.62
G3	23.51	23.46	24.13
NH1	58.99	59.24	59.19

E_{ZPE} is the ZPE-corrected electronic energy at 0 K while, E_{298} is the electronic + thermal energy and G_{298} is the free energy at room temperature. The relative energy values (kcal/mol) are given with respect to the most stable conformation N5 that has the following energies: $E_{ZPE} = -796.3024420$ a.u., $E_{298} = -796.286709$ a.u. and $G_{298} = -796.347071$ a.u.

the A conformers (protonation on the terminal amino group). The lowest-energy A-type configuration A6 already lies more than 5 kcal/mol above the absolute minimum energy conformer N5 and it is only the seventh lowest-energy structure. Its simulated spectrum does not fit well the experimental one: in particular, there is no line at 1295–1320 and 1595 cm^{-1}, and there is a doublet of extra lines at 1675 and 1715 cm^{-1} that does not clearly appear in the experiment. Among the N conformers, only the four lowest-energy structures, N5, N7, N2, and N1, seem to contribute to the experimental spectrum. The other configurations, N8, N4 and N10, possess too high energies, more than 5 kcal/mol above N5, and they display too many discrepancies in their IR spectrum, as illustrated with the N8 spectrum. The two lowest conformers, N5 and N7, possess very similar energies and rather similar structures, while the next two configurations, N1 and N2, lie about 3 kcal/mol above but are of different structures: N2 is similar to N5 and N7, with an H-bond between the protonated imidazole nitrogen and the carbonyl oxygen of the peptide bond, while this H-bond is made with the carboxylic acid oxygen in N1. As in AcNH-Ala, none of these conformers can account alone for the experimental data but each of them brings some features that do not appear in the others. For instance, many of the main experimental lines are present in the simulated N5 spectrum: the free acid C=O stretch calculated at 1786 cm^{-1}, the peptide C=O stretch strongly shifted down to 1615 cm^{-1} due to the protonated H-bond, and the free peptide N–H stretch calculated at 1522 cm^{-1}. On the other hand, the peak at 1740 cm^{-1} is lacking because it corresponds probably to the acid C=O stretch of conformer N1, which is red-shifted due to the H-bond with the protonated N–H group of imidazole and which is calculated at 1733 cm^{-1}. For this N1 conformer, the peptide C=O stretch is calculated to be weaker and located at 1693 cm^{-1} (very small feature in the experimental spectrum) and the peptide N–H stretch is calculated at 1498 cm^{-1}.

As in the previous section, if the conformer population would follow a simple Boltzmann law at room temperature, we could expect 77% for the N5 conformer, almost 23% for the N7 conformer and less than 0.2% for the N1 and N2 conformers. However, the above discussion about the simulated spectra suggests that conformer N1 noticeably contributes to the experimental spectrum. Again, this may be explain by the fact that ions are prepared at a high MALDI temperature and may not have enough time to really be equilibrated at room temperature, in our experimental conditions. However, high-energy conformers, i.e., lying more than 4 kcal/mol above the absolute minimum, are probably not present in the ion population since they do not bring any contribution to the IR spectrum. In the present case of protonated Ala-His, this means that the experimental spectrum is well interpreted in terms of the contribution of four dipeptides structures in which the protonation site is clearly on the imidazole nitrogen.

4. Conclusion

As expected from the proton affinities of the different amino acid sites, and as deduced from a comparison between experimental and simulated IR spectra, the extra proton is located on the peptide carbonyl oxygen in *N*-acetyl-alanine, and on the nitrogen of the imidazole side-chain in alanyl-histidine. However, in both cases, several equilibrium structures, which are calculating to lie less than 4 kcal/mol above the absolute minimum, seem to contribute to the experimental IRMPD spectrum. This is probably due to the high initial temperature of the MALDI process for ion production and to an incomplete thermalisation of the ions before IR absorption. The use of a softer ion production method and a more efficient cooling process, as it is achieved in radiofrequency trap apparatus with electrospray ionisation sources, would be desirable in order to obtain more thermally equilibrated species. However, the present experiments already reveal some information on the geometrical structures of the low-lying conformers of small protonated peptides.

References

[1] E.G. Robertson, J.P. Simons, Phys. Chem. Chem. Phys. 3 (2001) 1.
[2] B.C. Dian, J.R. Clarkson, T.S. Zwier, Science 303 (2004) 1169.
[3] M. Gerhards, C. Unterberg, A. Gerlach, A. Jansen, Phys. Chem. Chem. Phys. 6 (2004) 2682.
[4] W. Chin, M. Mons, J.P. Dognon, F. Piuzzi, B. Tardivel, I. Dimicoli, Phys. Chem. Chem. Phys. 6 (2004) 2700.
[5] I. Hünig, K. Kleinermanns, Phys. Chem. Chem. Phys. 6 (2004) 2650.
[6] P. Çarçabal, R.T. Kroemer, L.C. Snoek, J.P. Simons, J.M. Bakker, I. Compagnon, G. Meijer, G. von Helden, Phys. Chem. Chem. Phys. 6 (2004) 4546.
[7] B. Lucas, F. Lecomte, B. Reimann, H.D. Barth, G. Grégoire, Y. Bouteiller, J.P. Schermann, C. Desfrançois, Phys. Chem. Chem. Phys. 6 (2004) 2600.

[8] N. Hammer, J.W. Shin, J.M. Headrick, E.G. Dicken, J.R. Roscioli, G.H. Weddle, M.A. Johnson, Science 306 (2004) 675.
[9] N. Solca, O. Dopfer, J. Am. Chem. Soc. 126 (2004) 1716.
[10] K.R. Asmis, G. Meijer, M. Brümmer, C. Kaposta, G. Santambrogio, L. Wöste, J. Sauer, J. Chem. Phys. 120 (2004) 6461.
[11] R.L. Woodin, R.S. Bomse, J.L. Beauchamp, J. Am. Chem. Soc. 100 (1978) 3248.
[12] R.C. Dunbar, J. Chem. Phys. 95 (1991) 2537.
[13] S.A. McLuckey, D.E. Goeringer, J. Mass. Spectrom. 32 (1997) 461.
[14] J. Oomens, G. Meijer, G. von Helden, J. Phys. Chem. 105 (2001) 8302.
[15] J. Lemaire, P. Boissel, M. Heninger, G. Mauclaire, G. Bellec, H.N. Mestdagh, A. Simon, S.L. Caer, J.M. Ortega, F. Glotin, P. Maitre, Phys. Rev. Lett. 89 (2002) 273002.
[16] J. Oomens, D.T. Moore, G.V. Helden, G. Meijer, R.C. Dunbar, J. Am. Chem. Soc. 126 (2004) 725.
[17] D. Nolting, C. Marian, R. Weinkauf, Phys. Chem. Chem. Phys. 6 (2004) 2633.
[18] J.U. Andersen, H. Cederquist, J.S. Forster, B.A. Huber, P. Hvelplund, J. Jensen, B. Liu, B. Manil, L. Maunoury, S.B. Nielsen, U.V. Pedersen, J. Rangama, H.T. Schmidt, S. Tomita, H. Zettergren, Phys. Chem. Chem. Phys. 6 (2004) 2676.
[19] B. Paizs, M. Schnölzer, U. Warnken, S. Suhai, A.G. Harrison, Phys. Chem. Chem. Phys. 6 (2004) 2691.
[20] A. Simon, W. Jones, J.M. Ortega, P. Boissel, J. Lemaire, P. Maître, J. Am. Chem. Soc. 126 (2004) 11666.
[21] P. Maitre, S.L. Caer, A. Simon, W. Jones, J. Lemaire, H.N. Mestdagh, M. Heninger, G. Mauclaire, P. Boissel, R. Prazeres, F. Glotin, J.M. Ortega, Nucl. Instrum. Methods A 507 (2003) 541.
[22] B. Lucas, G. Grégoire, J. Lemaire, P. Maître, J.M. Ortega, A. Rupenyan, B. Reimann, J.P. Schermann, C. Desfrançois, Phys. Chem. Chem. Phys. 6 (2004) 2659.
[23] P.A. Schulz, A.S. Subdo, D.J. Krajnovitch, H.S. Kowk, Y.R. Shen, Y.T. Lee, Ann. Rev. Phys. Chem. 30 (1979) 379.
[24] K. Hakanson, H.J. Cooper, M.R. Hemmet, C.E. Costello, A.G. Marshall, C.L. Nilsson, Anal. Chem. 73 (2001) 4530.
[25] B. Paizs, I.P. Csonka, G. Lendvay, S. Suhai, Rapid Commun. Mass Spectrom. 15 (2001) 637.
[26] Z.B. Maksic, B. Kovacevic, Chem. Phys. Lett. 307 (1999) 497.